

Stop and restart of granular clock in a vibrated compartmentalized bidisperse granular system

Qi-Yi Liu,¹ Mao-Bin Hu,^{1,*} Rui Jiang,^{1,†} and Yong-Hong Wu²

¹*School of Engineering Science, University of Science and Technology of China, Hefei 230026, P.R. China*

²*Department of Mathematics and Statistics, Curtin University of Technology, Perth WA6845, Australia*

(Received 4 May 2012; revised manuscript received 13 December 2012; published 22 January 2013)

This paper studies a bidisperse granular mixture consisting of two species of stainless steel spheres in a vertically vibrated compartmentalized container. The experiments show that with proper vibration acceleration, the granular clock stops when horizontal segregation of the large spheres residing in the far end from the barrier wall occurs. When the segregation is broken, the granular clock restarts. We present the phase diagrams of vibration acceleration versus container width and small particle number, which exhibits three different regions, namely, clustering state, stop-restart of the granular clock, and the granular clock. A generalized flux model is proposed to reproduce the phenomenon of stop and restart of the granular clock.

DOI: [10.1103/PhysRevE.87.014202](https://doi.org/10.1103/PhysRevE.87.014202)

PACS number(s): 45.70.Mg, 45.70.Qj, 05.20.Dd

Introduction. Granular systems have attracted considerable attention, since they are intrinsically far from thermal equilibrium and therefore exhibit a host of pattern-forming instabilities such as surface waves [1–5] and segregation [6–10] [e.g., the Brazil Nut Effect (BNE), Reversed Brazil Nut Effect (RBNE), and Sandwich structure].

In granular gas, the loss of kinetic energy in collisions due to microscopic degrees of freedom of the system balances the energy gained from the shaking mechanism. This property makes the medium fundamentally different from any other ordinary molecular gas [11–22]. For monodisperse compartmentalized systems with strong driving, a uniform distribution appears. When the driving strength is reduced below a critical level, the particles cluster into one of the compartments. Eggers [11] proposed a prototype of a flux model to study this phenomenon: $\frac{dN_A}{dt} = -F_{A \rightarrow B} + F_{B \rightarrow A}$, where N_A denotes the number of particles in compartment A, and $F_{A \rightarrow B}$ ($F_{B \rightarrow A}$) is the particle flux from compartment A (B) to compartment B (A). Mikkelsen *et al.* studied a bidisperse granular gas, and they found that clustering can be directed either towards the compartment initially containing mainly large particles or to the one containing mainly small particles, by adjusting the vibration strength [12–14]. The Eggers flux model was extended as

$$\frac{dN_{i,A}}{dt} = -F_{i,A \rightarrow B} + F_{i,B \rightarrow A}, \quad (1)$$

where the subscript i denotes particle species.

A granular clock is an even more intriguing phenomenon observed in a bidisperse granular mixture, in which the clustering of particles between the compartments becomes periodic [16, 17, 19–22]. One possible origin of a granular clock is the BNE or RBNE. Hou *et al.* reproduced a granular clock in an experiment using particles of the same size. Therefore, it is supposed that the clock is driven by the oscillation of dual temperatures (i.e., two-particle species with different temperatures) [17, 23]. In a three-compartment system, Chen *et al.* reported a “granular follower” (extended clock) where

small spheres first move to one compartment, followed by large spheres [19]. In another study, they reported that an intruder will change the condensation temperature of granular gas and thus affect the granular clustering mode [21]. In an unequally compartmentalized system, Chen *et al.* reported two time periods: one for particles moving from the large compartment to the small compartment, and another for the reverse movement [22].

This paper reports experiment observations of a vertically vibrated bidisperse granular mixture in a wide system. In this system, horizontal segregation of the large spheres residing in the far end from the barrier wall might occur. Once this happens, the granular clock stops. When the segregation is broken, the granular clock restarts.

Experiment. The experiments are carried out in quasi-two-dimensional (2D) polystyrene chambers equally divided into two compartments with a short barrier wall. The base of the container is 1 cm in width and 12 cm in length. The short barrier wall is 3 cm in height and 0.3 cm in thickness. The thickness of the walls as well as the bottom of the container is also 0.3 cm.

We study a bidisperse granular mixture consisting of two species of stainless steel spheres; the diameter of large (small) spheres is $d_L = 5$ mm ($d_S = 2.5$ mm), and the number of large (small) spheres is $N_L = 20$ ($N_S = 200$). The container is vertically vibrated by an external shaker; and the frequency and amplitude of the vibration are adjustable through an input sinusoidal signal. An accelerometer is used to monitor the values of frequency and acceleration. A high-speed camera (480 Hz) and particle-tracking software are used to capture the flux of the spheres across the barrier.

In our experiments, the frequency is fixed at $f = 16.5$ Hz. As in the literature, when the vibration amplitude is large, spheres are uniformly distributed in the two compartments. With the decrease of amplitude, the granular clock is observed.

However, when the vibration acceleration decreases to the range $22\text{m/s}^2 \leq A \leq 26\text{m/s}^2$, a new phenomenon is observed. Figure 1 shows a typical time series of sphere proportions in the right compartment, where two modes (i.e., granular clock mode and clustering mode) are exhibited and the two modes appear alternatively.

*humaobin@ustc.edu.cn

†rjiang@ustc.edu.cn

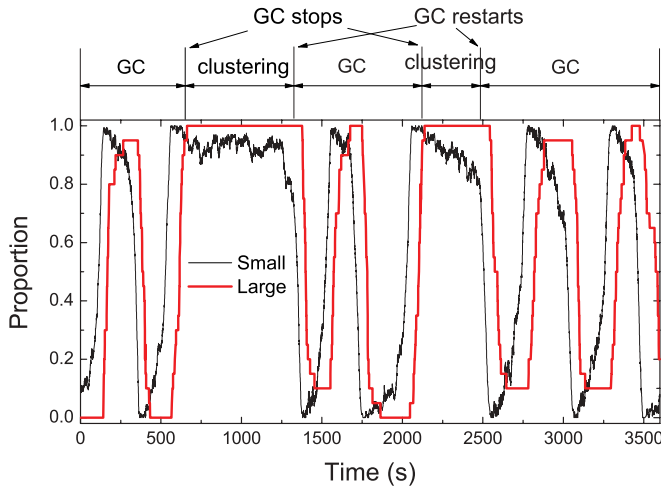


FIG. 1. (Color online) Typical experimental result showing a time series of small and large sphere proportions in the right compartment. GC stands for granular clock.

To illustrate the alternation phenomenon more clearly, we focus on the time interval from 2046 to 2776 s. Figure 2 shows several typical snapshots during this time period. At $t = 2046$ s [Fig. 2(a)], the system is in transient state in the granular clock mode. Almost all the small spheres have jumped into the right compartment, and the large ones are in the left compartment. Next, the large spheres follow the small ones and begin to jump to the right compartment. In the granular clock mode, once most of the large spheres have jumped into the right compartment, the small ones will be expelled and begin to jump back to the left compartment. However, the situation is different here. A close look at Fig. 2(b) shows that a horizontal segregation (type I) occurs with the large spheres residing in a zone near the far end from the barrier wall. This state is called clustering mode. In this mode, the horizontal segregation divides the compartment into a large sphere zone near the far end and a small sphere zone near the barrier. Since small spheres are likely to obtain more energy from collisions with large spheres, the small spheres could not gain enough energy to cross the barrier from the large sphere zone. Small spheres gaining momentum from the large sphere zone will soon be absorbed in the small sphere zone before crossing the barrier. As a result, the granular clock stops.

When this type of horizontal segregation appears, the large and small spheres are in dynamic balance: The large spheres tend to invade the small sphere zone, and the small spheres are usually able to expel them back [Fig. 2(c)]. Nevertheless, once the small spheres fail to expel the large ones back and the large spheres invade deep enough into the small spheres, the small spheres could gain enough energy from colliding with the large ones to jump across the barrier. Consequently, the granular clock restarts [Fig. 2(d)].

Figure 2(e) shows that at $t = 2546$ s, the granular clock reaches the symmetric state of Fig. 2(a). Then large spheres begin to jump to the left compartment. However, when most of the large spheres have jumped into the left compartment, a different type of horizontal segregation (type II) occurs, with the large spheres residing in the zone near the barrier wall [Fig. 2(f)]. As a result, small spheres could gain enough

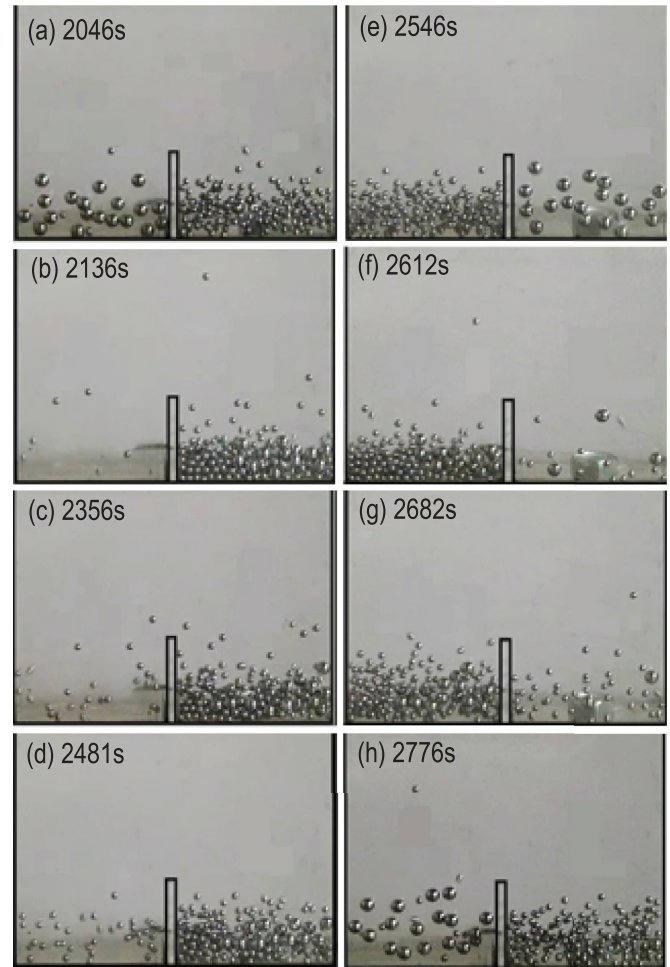


FIG. 2. (Color online) Snapshots of the vibrated bidisperse system. (a), (e), and (h) The transient state where large and small spheres are well separated; (b–d) the clustering mode that lasts for about 345 s; (e–h) the granular clock mode.

momentum from the large sphere zone and jump across the barrier due to the absence of the small sphere zone between the large sphere zone and the barrier. Therefore, the granular clock moves on [Figs. 2(g) and 2(h)]. Our experiments also found that in the granular clock mode, sometimes a mixture of spheres occurs instead of horizontal segregation of type II. In this case, the granular clock does not stop either.

Our experiments show that this phenomenon can be observed only when the acceleration is in an intermediate range. Figure 3 shows the phase diagrams of the system. The stop-restart of the granular clock appears within a crescent-like range of acceleration. When A is above the range, even if horizontal segregation of type I occurs, it will be broken very quickly. Therefore, the granular clock never stops. When A is below the range, the granular clock stops once the spheres accumulate in one compartment and never restarts. In Fig. 3(a), when the container width is very small (less than 6 cm), the stop and restart of the granular clock disappears because horizontal segregation cannot occur in the compartment. When the container width is sufficiently large (greater than 16 cm), the spheres become close to a monolayer so that horizontal segregation cannot develop either. One can also notice that

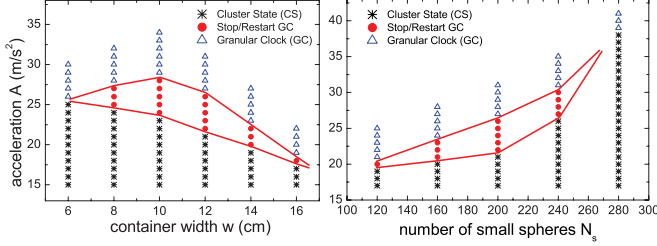


FIG. 3. (Color online) (a) Phase diagram of vibration acceleration vs container width. (b) Phase diagram of vibration acceleration vs small sphere number. The domain is divided by the Cluster State (CS), Stop-Restart of granular clock, and Granular Clock (GC). The solid lines are guide for the boundaries.

the lower boundary of the crescent-like region decreases with increasing container width. This is because the thickness of the granular layer decreases with container width. From the energy point of view, spheres can gain more energy from collisions with the base, and meanwhile, the energy dissipation decreases due to fewer intersphere collisions. Therefore, the system becomes more excitable, and the cluster state region shrinks accordingly.

Figure 3(b) shows the phase diagram of vibration acceleration a versus small particle number N_s . The stop and restart of the granular clock also appears within a crescent-like region. When $N_s < 120$, the large spheres will dominate and expel small spheres, so that the system easily enters the granular clock state. When there are too many small spheres ($N_s > 280$), horizontal segregation cannot develop because each large sphere is surrounded by small spheres. Therefore, the stop-restart of the granular clock also disappear. One can see that both the lower boundary and upper boundary increase as the number of small spheres increases. This is because more vibration energy is needed to excite the system. Therefore, the cluster state region expands with N_s .

In the clustering mode, the competition between the small sphere zone and the large sphere zone is crucial for the dynamics. Once the large spheres successfully invade the small sphere zone, the clustering period ends. In Table I we examine the lifetime of the clustering period in the stop-restart granular clock state. As the acceleration increases (for fixed container width $w = 12$ cm), the lifetime of the clustering period decreases monotonically. On the other hand, as the container width increases (for fixed acceleration $A = 26$ m/s²), the lifetime of the clustering period first increases and then decreases. The cluster lifetime will increase with small sphere number. For example, when the number of small spheres increases from 160 to 200 (fixed $A = 22$ m/s² and $w = 12$ cm), the lifetime increases from 560 to 676 s. When the number of

TABLE I. Average lifetime $\langle T_c \rangle$ of clustering mode.

Acceleration ($w = 12$ cm)	$\langle T_c \rangle$	Width ($A = 26$ m/s ²)	$\langle T_c \rangle$
22 m/s ²	676 s	8 cm	120 s
23 m/s ²	600 s	10 cm	202 s
24 m/s ²	480 s	12 cm	115 s
25 m/s ²	194 s		
26 m/s ²	115 s		

small spheres increases from 200 to 240 (fixed $A = 25$ m/s² and $w = 12$ cm), the lifetime increases from 115 to 800 s.

We have done experiments with two other different combination of sphere species, (1) [$d_L = 3.2$ mm, $d_S = 2.5$ mm, size ratio = 1.28], (2) [$d_L = 5.0$ mm, $d_S = 3.2$ mm, size ratio = 1.718], but no stop and restart of granular clock phenomenon is observed.

Flux model. With the experimental observation of horizontal segregation effect, we generalize the flux model [Eq. (1)] to simulate the stop and restart of the granular clock as follows:

$$\frac{dN_{i,A}}{dt} = -F_{i,A \rightarrow B} \zeta + F_{i,B \rightarrow A} \xi, \quad (2)$$

where the functions ζ and ξ are introduced to account for the influence of horizontal segregation on the fluxes. We set ζ and ξ as $\{0, 1\}$ binary functions. In particular, $\zeta = \xi = 1$ corresponds to the original flux model; $\zeta = 0, \xi = 1$ means that the clustering mode takes place with horizontal segregation of type I in compartment A, so that there is only $B \rightarrow A$ flux; $\zeta = 1, \xi = 0$ means the clustering mode with horizontal segregation of type I in compartment B, so that there is only $A \rightarrow B$ flux.

For the fluxes in Eq. (2), we adopt Hou's model [17], in which the barrier height has been taken into account. As a result, the model can be written as follows:

$$\frac{1}{K_{LA}} \frac{dN_{LA}}{dt} = -\frac{N_{LA}^2}{V_L(\chi_A)} e^{-a_L N_{LA}^2 / V_L^2(\chi_A)} \zeta + \frac{N_{LB}^2}{V_L(\chi_B)} e^{-a_L N_{LB}^2 / V_L^2(\chi_B)} \xi, \quad (3)$$

$$\frac{1}{K_{SA}} \frac{dN_{SA}}{dt} = -\frac{N_{SA}^2}{V_S(\chi_A)} e^{-a_S N_{SA}^2 / V_S^2(\chi_A)} \zeta + \frac{N_{SB}^2}{V_S(\chi_B)} e^{-a_S N_{SB}^2 / V_S^2(\chi_B)} \xi, \quad (4)$$

where N_{Si}, N_{Li} are numbers of small and large spheres in compartment i ($i = A, B$), which satisfy $N_{SA} + N_{SB} = N_s$, and $N_{LA} + N_{LB} = N_L$; K_{Si} and K_{Li} are constant parameters reflecting the material property of small or large spheres in compartment i ; $V_S(\chi_i)$ and $V_L(\chi_i)$ are estimations of small and large sphere velocities in compartment i , given by $V_S(\chi_i) = V_0/p(\chi_i)$, $V_L(\chi_i) = V_0/q(\chi_i)$. Here V_0 is the shaking velocity $V_0 = 2\pi af$, with a the amplitude and f the frequency of the vibration. The two functions $p(\chi_i)$ and $q(\chi_i)$ are adopted as $p(\chi_i) = 1 - 0.5 \exp(-\chi_i/\chi_0)$, and $q(\chi_i) = 1 + (\chi_i/\chi_0)^2$, with the sphere number ratios $\chi_0 = N_s/N_L$, $\chi_i = N_{Si}/N_{Li}$. The quantity a_s is expressed as $a_s = gh\pi d_s^4(1 - e^2)^2/\Omega^2$, where g is the gravity acceleration, h is the barrier height, d_s is the diameter of small sphere, e is the restitution coefficient of the spheres and is set to $e = 0.83$, and Ω is the bottom area of the compartment. Similarly, a_L is defined as $a_L = gh\pi d_L^4(1 - e^2)^2/\Omega^2$. This simulation uses $(N_s, N_L, d_s, d_L, \Omega, g, h, a, f) = (200, 20, 0.005, 0.0025, 0.00054, 9.8, 0.03, 0.0021, 16.5)$, which take the same values as in the experiment (MKS units). The constants $K_{LA} = K_{SA} = 0.0035$.

The evolution of ζ and ξ is defined as follows. Initially we set $\zeta = \xi = 1$, which corresponds to the granular clock mode. When most spheres gather in compartment A (in the simulation

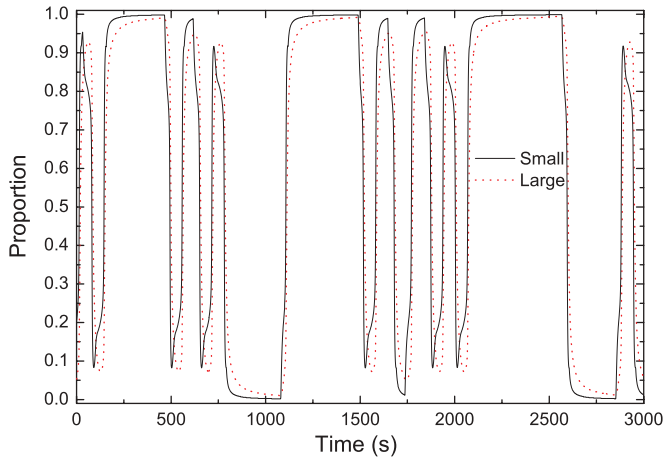


FIG. 4. (Color online) Time series of small and large sphere proportions in one compartment derived from theoretical simulation. The switch probabilities per unit time are $P_c = 10^{-2}\text{s}^{-1}$ and $P_r = 5 \times 10^{-5}\text{s}^{-1}$.

the criterion is set as $N_{LA}/N_L > 0.7$ and $N_{SA}/N_S > 0.7$), ζ is switched from 1 to 0 with a small switch probability per unit time P_c , which means that horizontal segregation of type I occurs in the compartment A and the system transits into the clustering mode. The parameter P_c thus determines the number of periods of the granular clock between two clustering modes. Then ζ is switched back from 0 to 1 with switch probability

per unit time P_r , which means that the horizontal segregation is broken and the system returns to the granular clock mode. The parameter P_r thus determines the lifetime of the clustering mode. Likewise, if $N_{LA}/N_L < 0.3$ and $N_{SA}/N_S < 0.3$ (most spheres have left compartment A), ξ is switched from 1 to 0 with switch probability per unit time P_c (horizontal segregation of type I occurs in compartment B). Then ξ is switched back from 0 to 1 with switch probability per unit time P_r . In simulation, the switch probability per unit time P_c (P_r) determines the switch probability $p_c(p_r)$ by $p_c = P_c \times \delta t$ ($p_r = P_r \times \delta t$), where δt is the time step of simulation, and $p_c(p_r)$ is the switch probability in one time step.

Figure 4 shows a typical time series of sphere proportions in one compartment derived from theoretical simulation. One can see that the model can successfully reproduce the stop and restart of the granular clock.

Conclusion. In summary, this paper studies a vertically vibrated bidisperse granular mixture in a wide compartmentalized container. Within a certain range of vibration acceleration, a granular clock could stop and restart. The dependence of the stop-restart granular clock phenomenon on experiment parameters is presented with the phase diagrams. A generalized flux model is introduced to reproduce the phenomenon.

Acknowledgments. We thank Prof. X. L. Gong for his assistance in the experiment. This work is funded by the National Natural Science Foundation of China with a Key Project No. 11034010.

-
- [1] T. Shinbrot and F. J. Muzzio, *Nature (London)* **410**, 251 (2001).
 - [2] P. Eshuis, K. van der Weele, D. van der Meer, R. Bos, and D. Lohse, *Phys. Fluids* **19**, 123301 (2007).
 - [3] H. J. van Gerner, M. A. van der Hoef, D. van der Meer, and K. van der Weele, *Phys. Rev. E* **82**, 012301 (2010).
 - [4] M. Rahman, K. Shinohara, H. P. Zhu, A. B. Yu, and P. Zulli, *Chem. Eng. Sci.* **66**, 6089 (2011).
 - [5] R. Akkerman, D. van der Meer, and D. P. van Donk, *Int. J. Prod. Res.* **48**, 3475 (2010).
 - [6] D. Brone and F. J. Muzzio, *Phys. Rev. E* **56**, 1059 (1997).
 - [7] E. A. Saied, *J. Stat. Phys.* **98**, 1395 (2000).
 - [8] X. Yan, Q. Shi, M. Hou, K. Lu, and C. K. Chan, *Phys. Rev. Lett.* **91**, 014302 (2003).
 - [9] Q. Shi, G. Sun, M. Hou, and K. Lu, *Phys. Rev. E* **75**, 061302 (2007).
 - [10] M. J. Metzger, B. Remy, and B. J. Glasser, *Powder Tech.* **205**, 42 (2011).
 - [11] J. Eggers, *Phys. Rev. Lett.* **83**, 5322 (1999).
 - [12] R. Mikkelsen, D. van der Meer, K. van der Weele, and D. Lohse, *Phys. Rev. Lett.* **89**, 214301 (2002).
 - [13] R. Mikkelsen, D. van der Meer, K. van der Weele, and D. Lohse, *Phys. Rev. E* **70**, 061307 (2004).
 - [14] K. Van der Weele, *Contemp. Phys.* **49**, 157 (2008).
 - [15] R. Lambiotte, J. M. Salazar, and L. Brenig, *Phys. Lett. A* **343**, 224 (2005).
 - [16] S. Viridi, M. Schmick, and M. Markus, *Phys. Rev. E* **74**, 041301 (2006).
 - [17] M. Hou, H. Tu, R. Liu, Y. Li, K. Lu, P. Y. Lai, and C. K. Chan, *Phys. Rev. Lett.* **100**, 068001 (2008).
 - [18] Y. Liu, Q. S. Mu, T. D. Miao, and J. H. Liao, *Europhys. Lett.* **84**, 14004 (2008).
 - [19] K. C. Chen, C. C. Li, C. H. Lin, L. M. Ju, and C. S. Yeh, *J. Phys. Soc. Jpn.* **77**, 084403 (2008).
 - [20] K. C. Chen, C. C. Li, C. H. Lin, and G. H. Guo, *Phys. Rev. E* **79**, 021307 (2009).
 - [21] K. C. Chen, W. L. Hsieh, and C. H. Lin, *Phys. Rev. E* **83**, 021303 (2011).
 - [22] K. C. Chen, C. H. Lin, and W. L. Hsieh, *Phys. Rev. E* **85**, 021306 (2012).
 - [23] Y. Li, R. Liu, and M. Hou, *Phys. Rev. Lett.* **109**, 198001 (2012).